EIGHTH INTERNATIONAL SYMPOSIUM ON APPLICATIONS OF LASER TECHNIQUES TO FLUID MECHANICS
July, 8 - 11, 1996, Lisbon, Portugal

MEAN AND TURBULENT FLOW CHARACTERISTICS OF SINGLE HYPERBOLOID IMPELLER STIRRED VESSELS

F. M. Piqueiro, M. F. Proença
Departamento de Engenharia Civil, Faculdade de Engenharia
Rua dos Bragas, 4099 Porto Codex, Portugal

F. T. Pinho
Departamento de Engenharia Mecânica e Gestão Industrial
Faculdade de Engenharia, Rua dos Bragas, 4099 Porto Codex, Portugal

A. M. Santos
Instituto de Engenharia Mecânica e Gestão Industrial, Unidade de Térmica Industrial
Rua do Barroco 174, 4465 S. Mamede de Infesta, Portugal

ABSTRACT

Detailed angle resolved measurements of the mean and rms velocities were carried out in a stirred vessel driven by a low power hyperboloid impeller with 8 shear ribs and 48 transport ribs at $1/10^{th}$ clearance from the bottom of the vessel.

In the turbulent flow regime the hyperboloid stirrer required only one fifth of the energy of more conventional agitators. In most in the vessel the fluid was found to flow axially downwards, with a velocity of around 5% of the tip velocity, and it raised close to the vessel walls reaching a maximum velocity of 15% of the tip velocity.

The turbulence was isotropic, with normalised rms values of 2% in the core of the vessel and growing up to 4% as the wall was approached. Flow periodicity was detected only at the vicinity of the impeller, in a region representing less than 5% of the whole volume of the tank, with rms velocities reaching maxima of 15% of the tip velocity.

1. INTRODUCTION

The search for energy savings and increased performance in stirred vessels has lead to the development of new impeller shapes, as is the case of the low power hyperboloid stirrer developed by Höfken *et al* (1991), a device that was designed for mixing sludges where the nitrification and oxigenation are important steps of the bacteriological digestion process.

The assessment of the quality of a mixing process requires a detailed knowledge of the flow characteristics within the stirred vessel and the quantification of some parameters, such as the local energy dissipation rate. Such information is especially important in the vicinity of the impeller, as shown by the research carried out over the years around the conventional Rushton impeller by Cutter (1966), Mujumdar *et al* (1987) and Laufhütte and Mersmann (1985) amongst others, and are required, for instance, for the proper development of computer codes.

Reed *et al* (1977) and Popiolek *et al* (1987) have measured the radial jet coming out of the Rushton impeller plane, colliding with the vessel wall and forming two wall jets. The latter authors characterised the large vortical structures coming out from behind the impeller blades into the bulk flow, above and below the impeller disc, with their angle-resolved measurements and have shown that not considering this flow periodicity would overpredict turbulent quantities by as much as 400%. The interaction between turbulence and the kinetics of aggregates in vessels stirred by Rushton turbines was investigated by Kusters (1991). Other investigations on the two- phase flow behaviour of the Rushton stirred vessel flow were those of Nouri and Whitelaw (1992).

Other standard impeller geometries, such as the pitched blade impeller, were also thoroughly investigated, as by Hockey (1990). He analysed in detail the flow characteristics of Newtonian and weakly elastic non- Newtonian fluids and quantified the distribution of the inputed energy into its various components, as a function of fluid rheology and impeller type.

Similar studies must obviously be performed with the new type of agitator, if it is to be well understood. Nouri and Whitelaw (1994) carried out some detailed velocity measurements with the hyperboloid impeller at the standard configuration of 1/3 clearance from the bottom, and conducted an overall assessment of the flow characteristics as a function of the impeller size and clearance. Their impeller included 8 shear ribs on the agitator upper surface, and they concluded that in terms of particle suspension effectiveness, the $1/10^{th}$ clearance impeller performed better than the 1/3 clearance impeller. The measured power consumption of the hyperboloid stirrer was at least 20 times lower than that of the Rushton impeller, although its Zwietering parameter was not so good. They demonstrated the advantage of mounting the impeller close to the bottom, with a $1/10^{th}$ clearance, but did not investigate in detail the flow characteristics of the hyperboloid stirrer with this low clearance, rather with the typical 1/3 clearance of conventional stirrers.

Some mixing processes require aeration, which for this impeller is usually introduced from its conical bottom surface, Höfken *et al* (1991). Their investigations on aerated systems led to an improved design of the impeller, with the incorporation of 48 transport ribs at the edge of the bottom surface, necessary for breaking up the gas bubbles. An efficient aeration from below the impeller also required it to be located close to the bottom of the vessel, in order to aerate the whole flow. So, for a number of reasons the $1/10^{th}$ clearance seems to be more adequate than other configurations and should be the object of research.

The objective of this work is the characterization of some of the mean and turbulent flow features in the stirred vessel powered by this low clearance hyperboloid agitator, having both the shear and transport ribs.

In the next section, the experimental facility, the instrumentation and the measuring programme are described. This will be followed by the presentation of the results and its discussion, and the paper will end with a summary of the main conclusions.

2. EXPERIMENTAL RIG

The stirred vessel had a diameter of 292 mm and the fluid height to vessel diameter ratio (H/T) was equal to 1. The hyperboloid stirrer was close to the bottom, at a clearance to vessel diameter ratio (C/T) of 1/10 and its diameter was equal to 100 mm, roughly corresponding to 1/3 that of the vessel diameter.

The vessel was mounted inside a square trough filled with the same liquid, in order to reduce optical refractions and help maintain a constant temperature in the bath, and the trough standed directly on top of a 3-D milling table for easy traversing.

Four 25 mm wide and 4 mm thick baffles were mounted inside of the tank, at 90° intervals, to avoid solid- body rotation of the fluid. They were not directly attached to the vessel wall, but were fixed to small triangular connectors, which separated them by 6 mm from the wall, thus eliminating the dead zones normally appearing behind the baffles. The bottom of the tank was flat and had a bearing embedded to support the drive shaft. A schematic representation of the vessel and the coordinate system used throughout this paper are shown in figure 1.

The hyperboloid stirrer was provided by Invent GmbH, according to its patented design and had 8 transport and 48 shear ribs on its top and bottom surfaces, respectively. The transport and shear ribs are small rectangles welded to the impeller surface at regular intervals, along their longer dimension. The transport ribs were 5.9 mm by 3.6 mm in shape and were mounted every 5°, and the shear ribs were 10 mm by 3.8 mm, and were mounted every 45°. The ribs were not aligned along

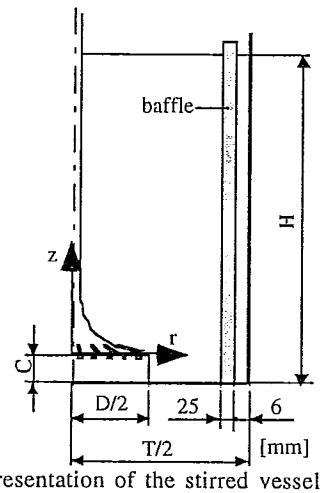

Figure 1- Representation of the stirred vessel and of the coordinate system.

diametral planes of the impeller, but had a 45° inclination in the horizontal plane. The construction was not perfect and there were rib to rib differences, especially with the transport ribs. More details on the construction can be found in Höfken and Bischof (1993). The stirrer was driven by a 600 W DC Servomotor controlled by a variable power supply unit, and the speed could be kept constant within 1 rpm, which corresponded to an uncertainty of less than 0.5%.

A one component Laser- Doppler anemometer from Dantec was used in forward scatter, whenever possible and in backscatter otherwise. The beam from the 100 mW Ar-ion laser, operating in multimode, passed through a series of optical elements before the Bragg cell, where a frequency shift of 0.6 MHz was imposed. To improve the alignment of the optics and reduce the size of the control volume, a pinhole section and beam expander, with an expansion factor of 1.95, were put before the 600 mm front lens.

The scattered light was collected by the photomultiplier (PM) before which stood an interference filter of 514.5 nm. The signal from the PM was processed by a TSI 1990 C counter operating in the single measurement per burst mode, with a frequency validation setting of 1% with 10/16 cycle comparison, after being band- pass filtered. A 1400 Dostek card interfaced the counter with a 80486 based computer, which provided all the statistical quantities, via a purpose built software.

For the angle resolved measurements, a mechanical encoder mounted on the shaft of the hyperboloid and connected to the counter, was used to discriminate the velocity measurements in 1° windows.

Due to the low velocities and high turbulence of this type of flows and in order to reduce the measuring uncertainties, a sample size of 30,000 realizations was selected for measurements taken far from the impeller, where the flow was not angle dependent. Close to the impeller, a total sample of 600,000 events was used, thus defining an average sample size of more than 1650 points per degree. In this region, weight average values of the mean and rms velocities were also calculated from the 1° angle-resolved data, to allow a proper visualisation of the mean flow field. These weight-average mean and rms values were calculated using equations 1 and 2, respectively.

$$\overline{U} = \frac{\sum_{\theta=1}^{360} U_\theta N_\theta}{\sum_{\theta=1}^{360} N_\theta} \qquad (1)$$

$$\overline{u'^2} = \frac{\sum_{\theta=1}^{360} \overline{u'^2}_\theta N_\theta}{\sum_{\theta=1}^{360} N_\theta} \qquad (2)$$

where U_θ, $\overline{u'^2}_\theta$ and N_θ represent local angle- resolved values of the mean velocity, variance of the velocity and sample size, respectively.

Table 1 lists the main characteristics of the LDA system, and an assessment of the various contributions to the overall uncertainty of the mean and rms velocities

Table 1- Main characteristics of the Laser- Doppler anemometer in air at e^{-2} intensity.

Laser wavelength	514.5 nm
Measured half angle of beams in air	3.65°
Dimensions of measuring volume in air	
major axis	2.53 mm
minor axis	162 μm
Fringe spacing	4.041 μm
Frequency shift	0.6 MHz

gave the following results: for the 360° ensemble average measurements taken far from the impeller, the overall uncertainty of the mean velocity is thus less than 1.2% for a 100% turbulence intensity and of about 5% for the rms velocity, in regions of high turbulence. Close to the agitator, with the average sample size of 1650 points per degree, the overall uncertainty was less than 3.5% and 5% for the mean and rms velocities, respectively, also under conditions of 100% turbulence intensity.

3. RESULTS AND DISCUSSION

Figure 2 compares the power consumption of the hyperboloid stirrer with that of the Rushton and pitched blade impellers, over the laminar and turbulent flow regimes. There is a clear energy advantage of the hyperboloid stirrer for Reynolds numbers above 50, because of the early transition to turbulence and flow separation of the Rushton and pitched blade impellers. However, for lower Reynolds numbers the flow is not separated and the hyperboloid impeller requires more power, because of the friction over its larger surface area. These observations are well documented and explained in Piqueiro *et al* (1995).

Most of the current practical applications of the hyperboloid stirrer are for turbulent flow conditions, hence a Reynolds number of 50,000, where the power curve has stabilised, was selected for the detailed flow field investigation reported here.

Next, the mean flow characteristics are presented and discussed and are followed by those of the turbulent flow field. After this overall picture, the paper moves on to discuss the periodic flow near the impeller and the bottom of the vessel. All the velocities were normalised with the impeller tip velocity and the values of the radial locations by the impeller radius. The axial coordinate was left in [mm], because we felt it was easier to visualize the flow in this way. We remind the reader that the vessel height is 300 mm, the impeller radius is 50 mm and the shear rib height is 5 mm.

The vertical cut through a radial plane in figure 3 shows a vector plot of the mean axial and radial velocity components, whereas figures 4 a), b) and c) and figures 5 a), b) and c) show radial profiles of the mean axial, radial and tangential velocity components. These figures were made from the measured 360° ensemble-average data taken far from the impeller and weighted averages calculated from the angle resolved measurements close to the impeller.

The flow is predominantly a downward axial flow, with an average magnitude of about 5% of the tip velocity, occupying over 70% of the radius of the vessel. Then, mass conservation requires a rather strong upwards

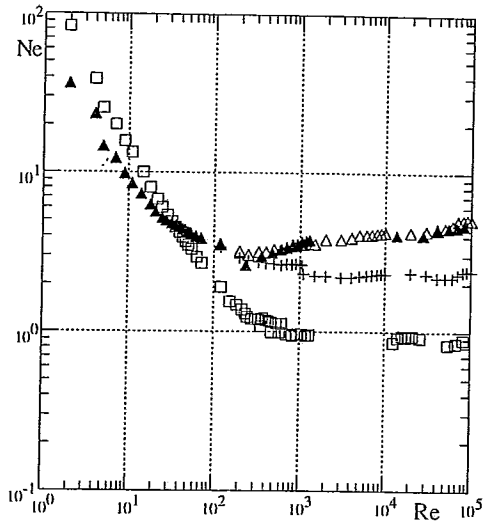

Figure 2- Newton number versus Reynolds number for H/T=1 and D/T=1/3. Comparison with the literature. This work: □ hyperboloid; ▲ Rushton. From Hockey (1990): △ Rushton and + pitched blade.

axial flow close to the vessel side wall, reaching a maximum of 15% of the tip velocity. Near the tip of the impeller, the long vectors show that the velocities are very intense because the flow is being pushed directly by the ribs.

A radial velocity component is acquired only very close to the impeller surface, and especially at the bottom of the vessel. On the upper half of the vessel (z> +140 mm) the fluid moves slowly towards the shaft, with a magnitude of about 2% of the tip velocity, whereas the outwards radial flow between z= +20 to z=+90 mm is also of about 2% of the tip velocity. Further down, close to the bottom, in a region also influenced by the agitator, the radial velocities are higher than above, reaching maximum values of about 10% of the tip velocity, and at the impeller, where the fluid is being pushed by the shear ribs, of 20 to 30% of the tip velocity.

The vortex defined by the circulating flow pattern just described is centred at around r/R = 2.4 and z/R = 1.75.

Close to the free surface (z> +190 mm), but especially above z = +240 mm, the measured axial and radial velocity components tend to zero, i.e., the fluid is almost motionless.

The mean tangential velocity component has magnitudes similar to the mean radial velocity component, except near the impeller. Far from the agitator the fluid slowly rotates in the same direction of the impeller, with magnitudes between 1 to 4% of the tip velocity. It is below the impeller that the rotational velocities are higher because of the transport ribs, but they decrease very quickly with the radius, dropping from over 40% of the tip velocity at r/R= 1.08 to less than 10% at r/R=1.4.

Below the impeller the rotation of the fluid is always positive but not above its base plane. Here, starting at about r/R= 1.5 and up to the vessel side wall, the fluid rotates in the opposite direction to the impeller, with the higher negative velocity, of around 2.5% of the tip velocity, occurring close to the wall. This counter-rota-

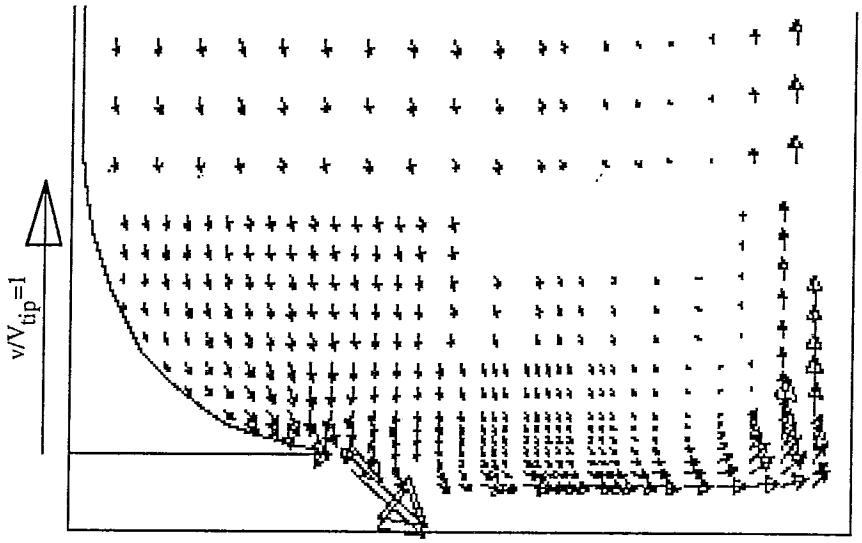

Figure 3- Vector plot of the mean axial and radial velocity components in a diametral vertical plane in the vicinity of the bottom of the vessel and impeller.

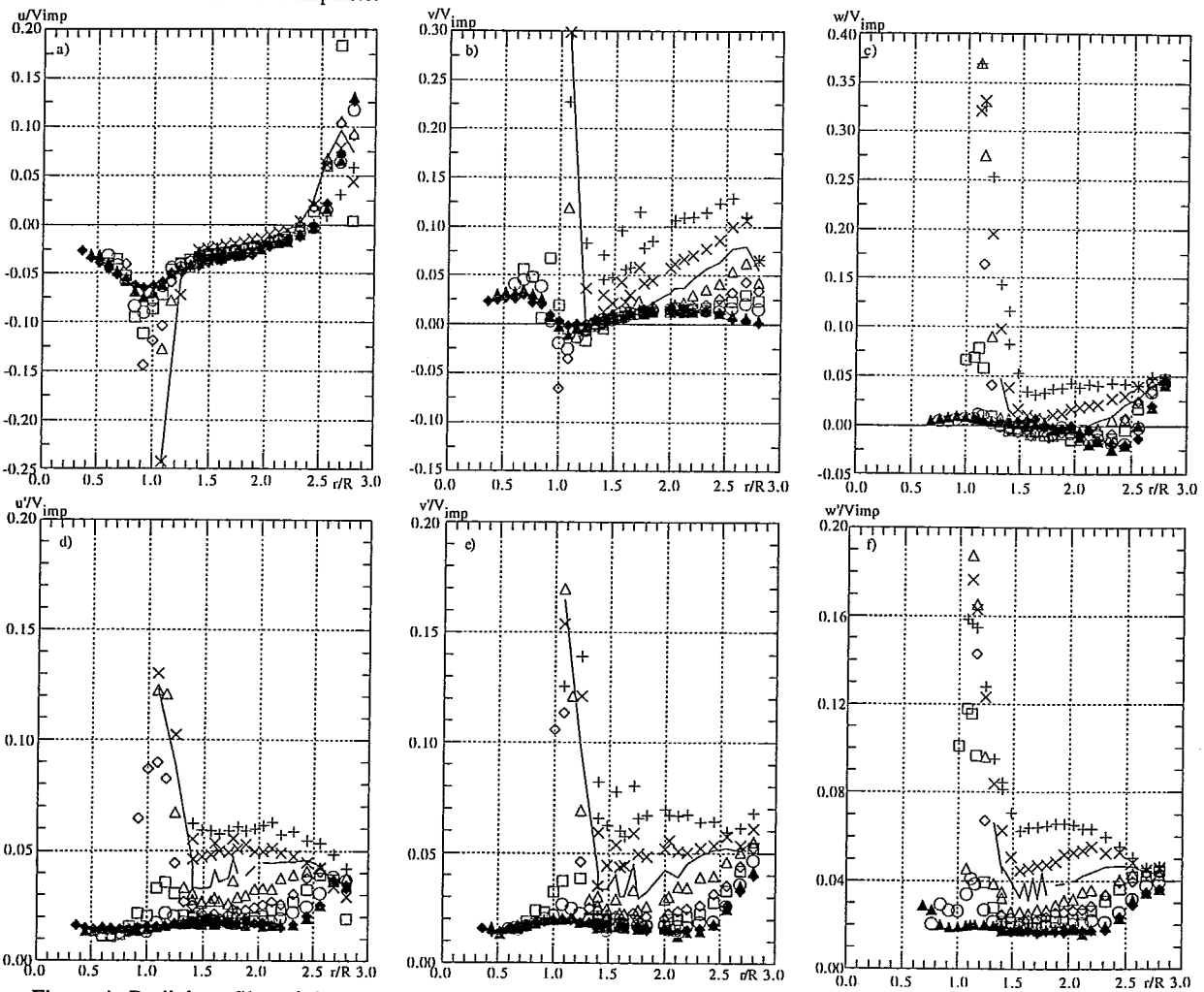

Figure 4- Radial profiles of the normalised mean and rms axial (u), radial (v) and tangential (w) velocity components at different heights. + z=-5, x z=-3, — z=-1, Δ z=+1, ◊ z=+3, □ z=+5, o z=+7, ▲ z=+11, ♦ z=+15.

ting flow disappears for heights above 60 mm from the impeller base plane, and could be due to the simultaneous influence of the baffles and a low pressure created by the high speed jet at the bottom.

Figures 4d), e) and f) and figures 5 d), e) and f) represent radial profiles of the normalised rms of the axial, radial and tangential· velocity components at different heights. As far as the turbulence is concerned two different zones are distinguished. Above z=+7 mm the turbulence is isotropic and remains fairly constant, regardless of the vessel height, at about 2% of the tip velocity in the center of the vessel, growing to 4% near the side walls.This higher turbulence is due to turbulence production on the side wall jet, plus a contribution of transported turbulence by this jet, which originated from the high turbulence radial flow at the bottom of the vessel. Near the free surface, the slow velocities reduce the turbulence to values of about 1 to 1.5% of the tip velocity.

Below z=+7 mm the turbulence continues to be rather isotropic, but here it is high because of the proximity of the impeller and of the bottom of the vessel. At the impeller the high shear rates created by the passage of the ribs are an important contribution to the production of turbulence, whereas at the bottom of the vessel the turbulence is produced at the boundary-layer created by the radial disharge jet.

The 8 shear ribs located above the impeller base plane (z=0) create· local flow reversals relative to the mean vectors plotted in figure 3, and a strong periodic flow emanates from that region. However, this periodicity is rather short- lived in comparison to that in more typical agitators, such as the Rushton and pitched-blade impellers of Hockey (1990).

Note also, that a strong radial flow does not exist at the impeller base plane, but below it. Unfortunately, due to difficulties in measuring close to the bottom, detailed velocity measurements have not yet been carried out here, but the increase in the magnitude of the vectors in the radial direction at the lowest measured horizontal plane, as one approaches the vessel side walls, suggests that closer to the bottom the radial velocities could be even stronger, with a boundary-layer type flow growing to the outside.

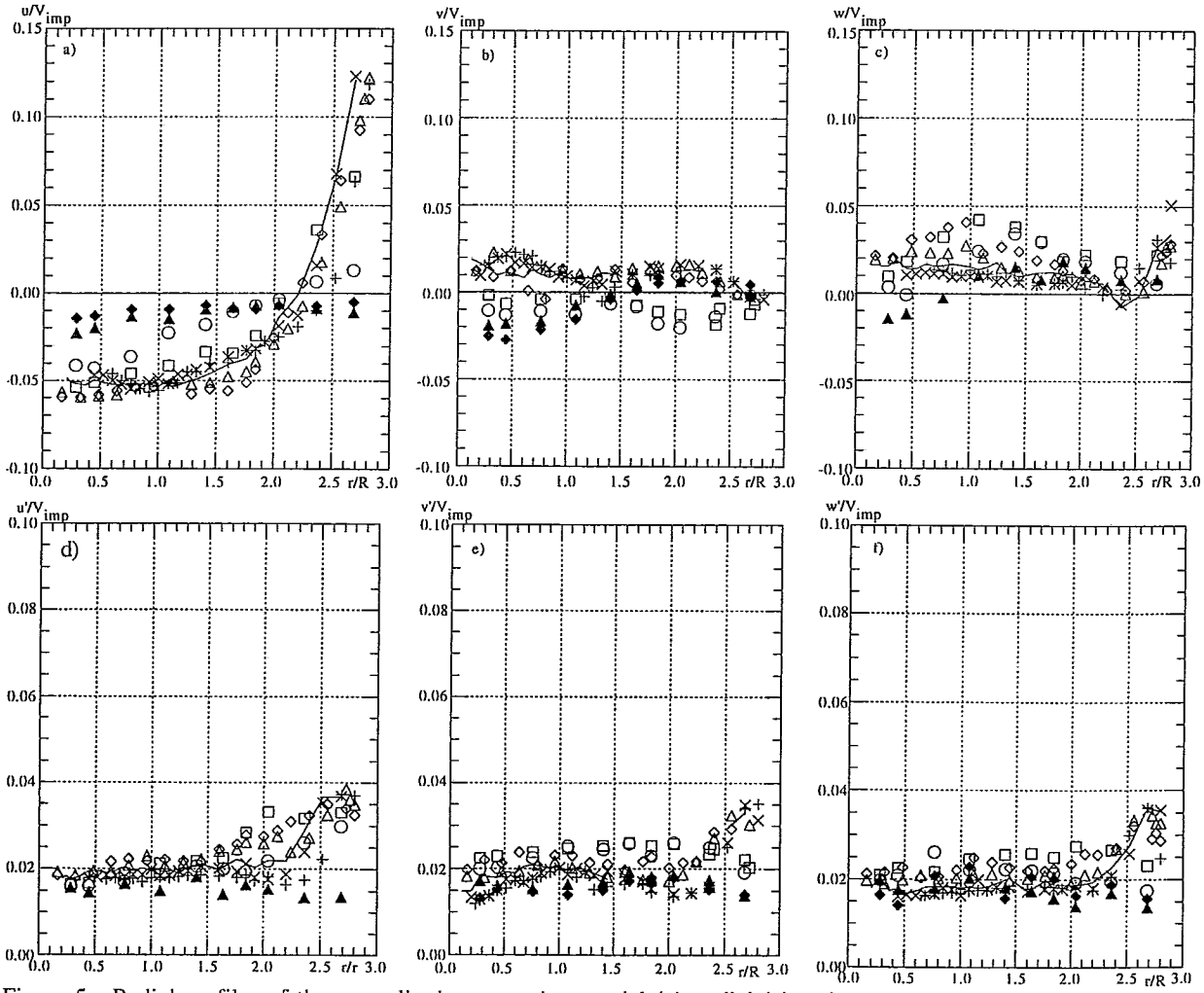

Figure 5- Radial profiles of the normalised mean and rms axial (u), radial (v) and tangential (w) velocity components at different heights. + z=+20, x z=+25, — z=+40, Δ z=+60, ◊ z=+90, □ z=+140, o z=+190, ▲ z=+240, ◆ z=+270.

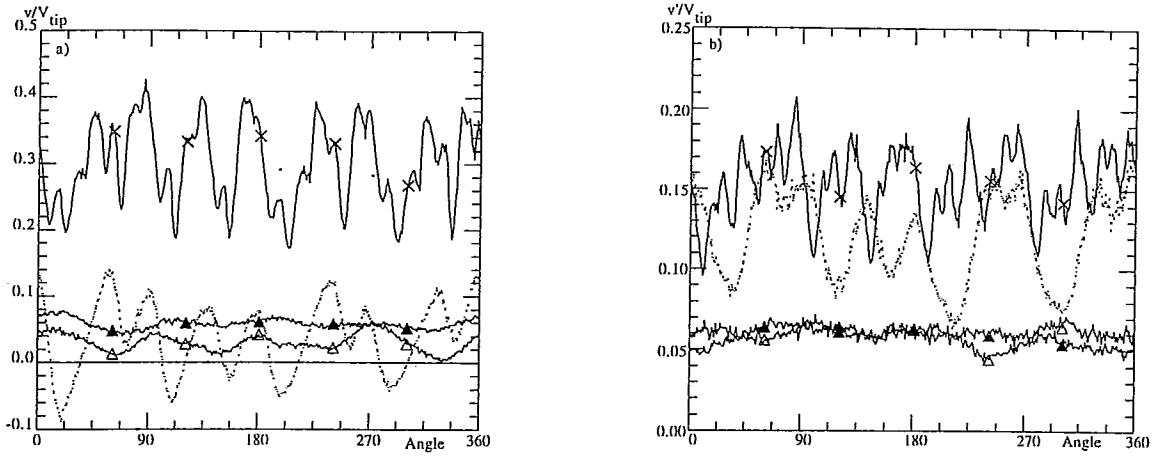

Figure 6 a) and b) Mean and rms radial velocity component at z= -3 mm as a function of the angular position and at radial locations: r/R= 1.08 -X-, r/R= 1.24 ----, r/R= 1.4 -Δ- and r/R= 1.76-▲-.

The most interesting flow features are those near the impeller tip, where the periodicity imposed by the shear and transport ribs is felt. In terms of periodicity three different flow patterns are identified, corresponding to three different regions, one below the impeller base plane and two above.

Below the impeller base plane, the flow is affected by both the 8 shear ribs and the 48 transport ribs, with this combination imparting a rather chaotic flow behaviour, as one of the angular plots of figure 6 shows. This figure presents four different profiles of the radial velocity component at four different radial locations pertaining to the same horizontal plane, located below the impeller. The eight major cycles at r/R = 1.08 are disturbed by the strong tangential flow created by the 48 ribs, which tend to smooth out the periodicity imposed by the shear ribs, a more clearly noticed effect in the rms velocity profile than in the mean velocity profile. Moving away from the impeller the effect of the ribs is reduced, so that at r/R= 1.24 the eight cycles still exist with a lower amplitude and especially with less "noise", from the transport ribs.

Farther away from the agitator, the reduction of the flow periodicity occurs through a pairing process, which led to the formation of only four low- amplitude cycles at r/R = 1.4. The curves pertaining to r/R= 1.08 and 1.24 are also seen to decay, on the average, to values of about 5% of the tip velocity, as we move into a zone of stronger axial flow. At a higher radius (r/R = 1.76) the periodicity has been reduced to a small single cycle, an effect which we attribute to the small wobbling of the impeller.

Above the impeller base plane, at the plane touching the upper edge of the shear ribs, the flow exhibits a strong eight- cycle periodicity, with the observed cycle to cycle differences always taking place at the same location, i.e., they seem to be attributed to imperfections in the positioning of the ribs on the impeller upper surface.

Figure 7 shows a typical 360° angular profile with such cycle-to-cycle differences. The eight measured cycles were averaged into a single 45° cycle and this average profile was reproduced to the full 360° in the figure, for assessing the magnitude of the cycle- to- cycle differences. These differences are more intense in the 5th and 6th cycle, and in the rms of the velocity than in the mean velocity, being at most of 30% and 20% in the magnitude, respectively. The stronger effect upon the rms is expected, because of its strong dependence of the shear

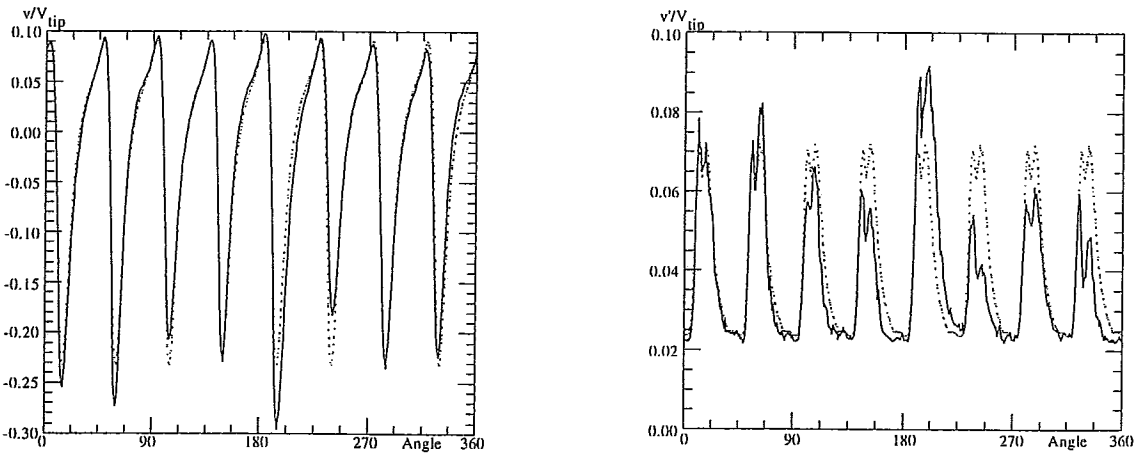

Figure 7 a) and b) Angular profiles of the mean and rms normalised radial velocities at z=+ 5 mm and r/R= 1.08. Solid line: measured profile. Broken line: calculated average cycle.

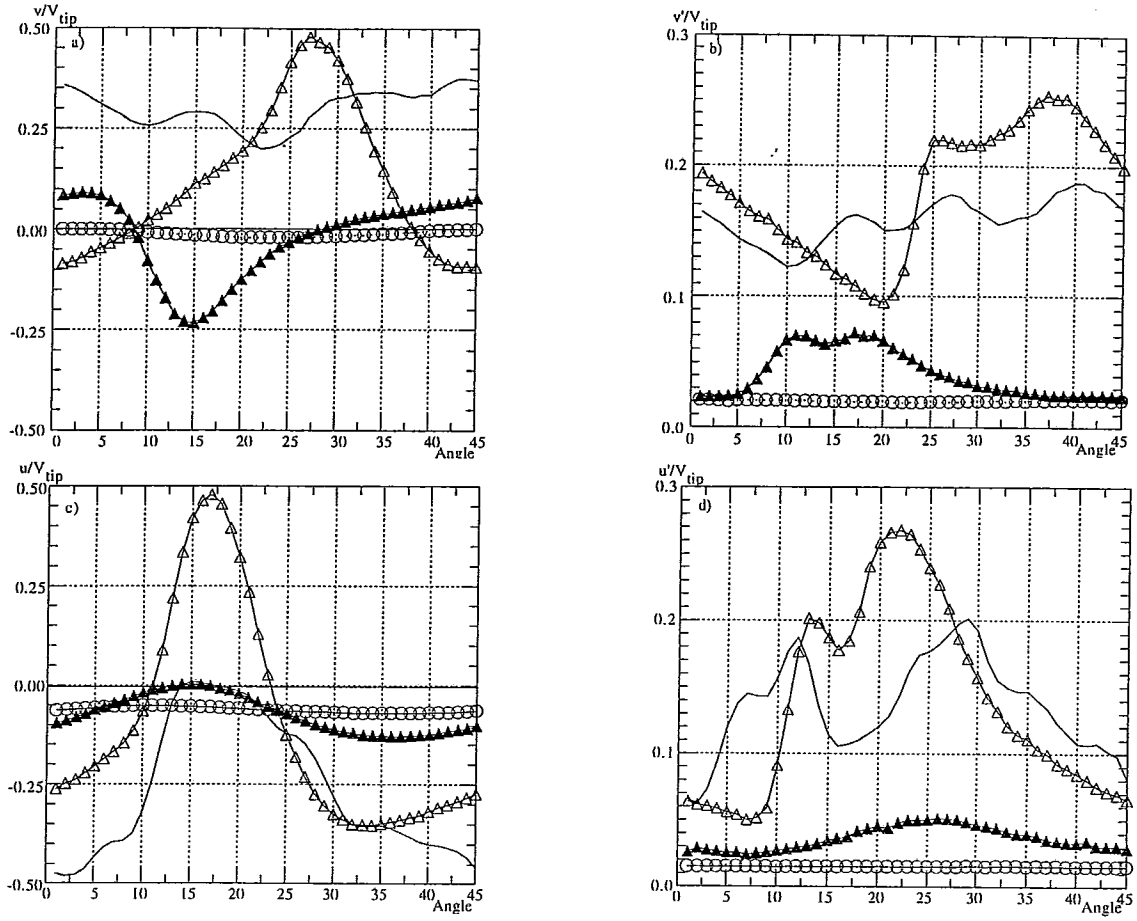

Figure 8 Angular profiles of the mean and rms radial (v) and axial (u) velocity components at z= -3 mm (—), z= +1 mm (Δ), z= +5 mm (▲) and z= + 11 mm (O), for a constant r/R= 1.08.

rates. Since the amplitudes of the mean velocity cycles are large, slight imperfections in the construction change the maximum shear rate and thus the rms of the velocity value.

Close inspection of the impeller showed that the 6th shear rib, located at 225°, was slightly bent forward rather than being perpendicular to the impeller surface and could be responsible for the two different cycles which stand between 180° and 270°. The gentle wobble of the impeller motion and other minor imperfections could then be behind the other smaller variations.

In the remaining of the paper, the description of some of the characteristics of the periodic flow is based on the calculated 45° average cycle rather than on the fully measured 360° angular profile.

In figure 8, angular profiles of the radial and axial mean and rms velocity components, pertaining to points at the same radial location r/R= +1.08, but to different heights, below and above the impeller base plane, are plotted. The figure confirms that below the impeller, the outwards radial velocity is fairly constant, because of the smoothing effect of the strong tangential flow induced by the transport ribs, whereas above the agitator the periodicity is better defined.

The strong periodicity introduced by the shear ribs is not only found in the angle dependence, but also in the vector direction. Comparing the mean velocity profiles pertaining to z= +1mm (aligned with the root of the rib) and z=+5 (aligned with the upper edge of the rib) four dif-

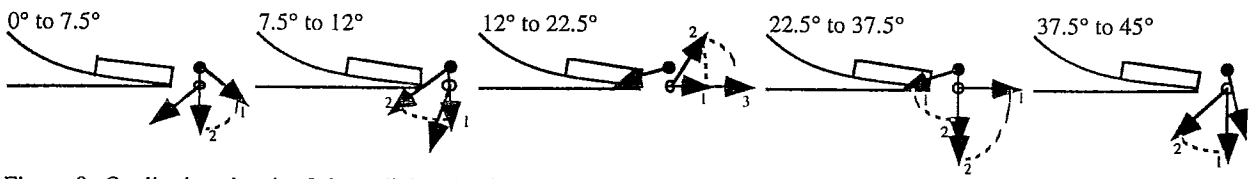

Figure 9- Qualitative sketch of the radial and axial mean flow pattern close to the ribs, as a function of the angular location. θ= 0° and θ= 45° are the locations of consecutive tips of shear ribs.

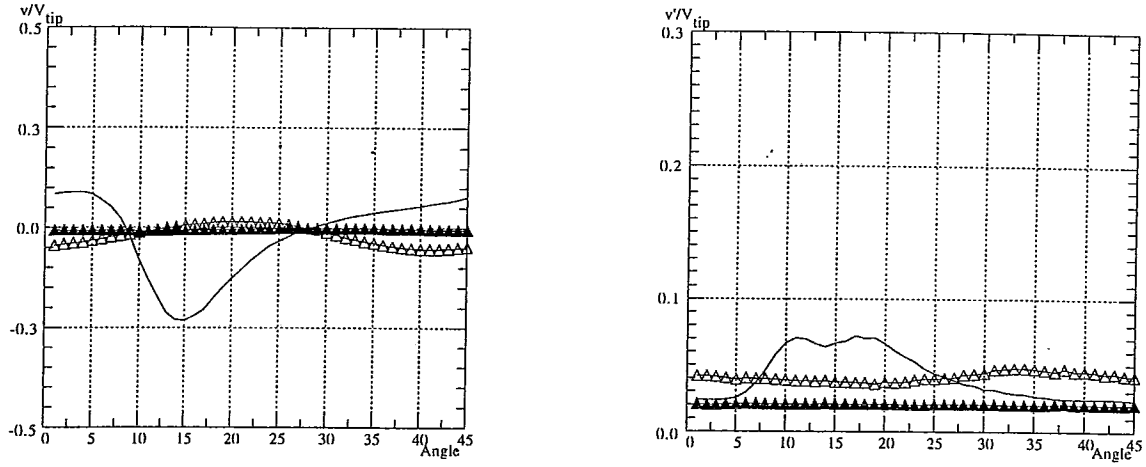

Figure 10 a) and b) Mean and rms radial velocity component at r/R= 1.08 (—), r/R= 1.24 (Δ) and r/R= 1.4(▲) as a function of the angular position at z= +5 mm.

ferent types of behaviour are identified, which are qualitatively sketched in figure 9. The flow has been described on average as going down axially and outwards radially, but close inspection of figure 8 shows that in between the ribs, there are instances when the fluid flows the other way around, i.e., upwards and towards the impeller, rather than away from it.

Figure 10 shows angular profiles of the normalised radial component of the velocity at different radius and at a constant height of z= +5 mm, and together with figure 8 it allows the assessment of the extent of the zone of influence of the rib- induced periodicity. Since the flow is on the whole an axial downwards flow, it is not surprising to observe that above the impeller the region affected by the ribs is very limited, and that at r/R= 1.4 the flow remains independent of the angle.

From data not presented here, we observed that the vertical influence was also rather limited to about three rib heights, i.e., at z=+15 mm the periodic flow was barely noticed. Obviously, considering the mean flow patterns presented and discussed above, the region of periodic flow below the impeller is longer, going up to about r/R= 1.76. Thus, the volume of fluid experiencing periodic effects above and below the impeller base plane account for less than 5% of the total volume of the vessel.

4. CONCLUSIONS

Detailed angle- resolved measurements of all three components of the mean and rms velocities in a stirred vessel, powered by a low consumption hyperboloid stirrer, were carried out using laser- Doppler anemometry, after measurements of the torque allowed the definition of the power consumption curve.

The hyperboloid stirrer was found to require only one fifth of the energy of conventional stirrers (Rushton and pitched blade) for Reynolds numbers above 1 000, but was less efficient for Reynolds numbers under 200.

The flow field was mainly axial, with a downwards velocity of about 5% of the tip velocity in the central part of the tank, and a wall jet up the side walls with a maximum mean velocity of around 15% of the tip velocity. In the same regions the turbulence was isotropic with an intensity of about 2% and growing up to 4%, respectively. The flow was three-dimensional, but quite uniform in all components, without strong shear rates except in the close vicinity of the shear ribs. However, this and other parameters still need to be quantified for comparison with those of conventional agitators. No dead zones were encountered within the vessel, making this impeller adequate for applications were a full gentle motion of the fluid, without excessive local deformation rates, is required.

Periodicity in the mean and turbulent flow fields was limited to less than 5% of the volume of the tank, and was found only close to the impeller and at the bottom of the vessel. The main periodicity was introduced by the 8 shear ribs on the upper surface of the impeller, whereas the 48 transport ribs at its bottom surface were mainly responsible for increasing the turbulence at the bottom, inducing a strong tangential flow and smearing the strong 8- cycle periodic flow, thus introducing a rather chaotic flow behaviour. Within this region, maximum values of the rms velocity of around 25% of the tip velocity were measured.

Further analysis of the data is required to extract various other useful quantities needed for assessing the performance of this impeller, such as the pump discharge coefficient and the distribution of the energy input into its various forms.

ACKNOWLEDGEMENTS

The authors wish to thank the European Commission and Junta Nacional de Investigação Científica e Tecnológica for financing this work through contracts JOU 2-CT9-0127 and PEAM/C/TAI/265/93, respectively. Special thanks are due to Mrs. Manuela Lemos for her assistance and valuable comments and to Mr. Jerónimo de Sousa for his technical support.

REFERENCES

Cutter, L. A. 1966. Flow and turbulence in a stirred tank. AIChEJ, vol. 12, pp. 35- 45.

Durst, F., Melling, A. and Whitelaw, J. H. 1981. Principles and Practice of Laser- Doppler Anemometry, 2nd Edition, Academic Press.

Hockey, R. M. 1990. Turbulent Newtonian and non-Newtonian flows in a stirred reactor. PhD Thesis, University of London, London.

Höfken, M., Bischof, F. and Durst, F. 1991. Novel hyperboloid stirring and aeration system for biological and chemical reactors. ASME FED- Industrial Applications of Fluid Mechanics, vol. 132, pp.47- 56.

Höfken, M. and Bischof, F. 1993. Hyperboloid stirring and aeration system: operating principles, application, technical description. Invent GmbH report, version 1.1, August 1993, Erlangen.

Kusters, K. A. 1991. The influence of turbulence on aggregation of small particles in agitated vessels. PhD Thesis, Technical University of Eindhoven.

Laufhüttle, H. D. and Mersmann, A. B. 1985. Dissipation of the power in stirred vessels. 5th European Conference on Mixing, Würzburg, West Germany, 10- 12 June, Paper 33, pp 331- 340.

Melling, A. 1975. Investigation of Flows in Non-Circular Ducts and Other Configurations by Laser-Doppler Anemometer. PhD Thesis, Imperial College, University of London.

Mujumdar, A. S., Huang, B., Wolf, D., Weber, M. E. and Douglas, W. J. M. 1970. Turbulence parameters in a stirred tank. Can. J. Chem. Eng., vol. 48, pp.475- 483.

Nouri, J. M. and Whitelaw, J. H. 1992. Particle velocity characteristics of dilute to moderately dense suspension flows in stirred reactors. Int. J. Multiphase Flow., vol. 18, pp. 21-33.

Nouri, J. M. and Whitelaw, J. H. 1994. Flow characteristics of hyperboloid stirrers. Can. J. Chem. Eng., vol. 72, pp. 782- 791.

Piqueiro, F. M., Valente, J. T. and Pinho, F. T. 1995. Power consumption and flow pattern of the mixing vessel flow with single and double hyperboloid stirrers. Internal report, Deps. Civil and Mech. Eng., Faculty of Engineering, University of Porto, Portugal.

Popiolek, Z., Yianneskis, M. and Whitelaw, J. H. 1987. An experimental study of steady and unsteady flow characteristics of stirred reactors. J. Fluid Mech., vol. 175, pp. 537- 555.

Reed, X. B., Princz, M. and Hartland, S. 1977. Laser-Doppler measurement of turbulence in a standard stirred tank. Proc. 2nd Euro Conf. Mixing, Cambridge, UK, paper B1, 1.

T. S. I. 1988. Manual of the 1990 C counter, TSI Incorporation, Minneapolis.

Vafidis, C. 1985. Aerodynamics of Reciprocating Engines. PhD Thesis, Imperial College, University of London.

Yanta, W. J. and Smith, R. A. 1973. Measurements of Turbulence- Transport Properties with a Laser- Doppler Velocimeter. 11th Aerospace Science Meeting, Washington, AIAA paper 73, pp. 169-180 .

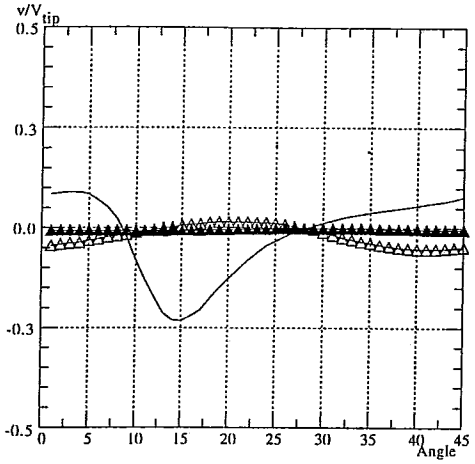

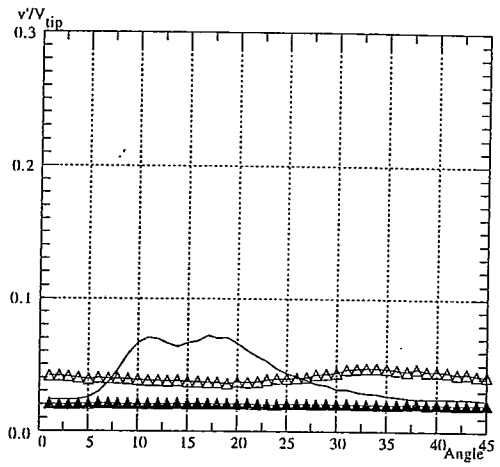

Figure 10 a) and b) Mean and rms radial velocity component at r/R= 1.08 (—), r/R= 1.24 (Δ) and r/R= 1.4(▲) as a function of the angular position at z= +5 mm.

ferent types of behaviour are identified, which are qualitatively sketched in figure 9. The flow has been described on average as going down axially and outwards radially, but close inspection of figure 8 shows that in between the ribs, there are instances when the fluid flows the other way around, i.e., upwards and towards the impeller, rather than away from it.

Figure 10 shows angular profiles of the normalised radial component of the velocity at different radius and at a constant height of z= +5 mm, and together with figure 8 it allows the assessment of the extent of the zone of influence of the rib- induced periodicity. Since the flow is on the whole an axial downwards flow, it is not surprising to observe that above the impeller the region affected by the ribs is very limited, and that at r/R= 1.4 the flow remains independent of the angle.

From data not presented here, we observed that the vertical influence was also rather limited to about three rib heights, i.e., at z=+15 mm the periodic flow was barely noticed. Obviously, considering the mean flow patterns presented and discussed above, the region of periodic flow below the impeller is longer, going up to about r/R= 1.76. Thus, the volume of fluid experiencing periodic effects above and below the impeller base plane account for less than 5% of the total volume of the vessel.

4. CONCLUSIONS

Detailed angle- resolved measurements of all three components of the mean and rms velocities in a stirred vessel, powered by a low consumption hyperboloid stirrer, were carried out using laser- Doppler anemometry, after measurements of the torque allowed the definition of the power consumption curve.

The hyperboloid stirrer was found to require only one fifth of the energy of conventional stirrers (Rushton and pitched blade) for Reynolds numbers above 1 000, but was less efficient for Reynolds numbers under 200.

The flow field was mainly axial, with a downwards velocity of about 5% of the tip velocity in the central part of the tank, and a wall jet up the side walls with a maximum mean velocity of around 15% of the tip velocity. In the same regions the turbulence was isotropic with an intensity of about 2% and growing up to 4%, respectively. The flow was three-dimensional, but quite uniform in all components, without strong shear rates except in the close vicinity of the shear ribs. However, this and other parameters still need to be quantified for comparison with those of conventional agitators. No dead zones were encountered within the vessel, making this impeller adequate for applications were a full gentle motion of the fluid, without excessive local deformation rates, is required.

Periodicity in the mean and turbulent flow fields was limited to less than 5% of the volume of the tank, and was found only close to the impeller and at the bottom of the vessel. The main periodicity was introduced by the 8 shear ribs on the upper surface of the impeller, whereas the 48 transport ribs at its bottom surface were mainly responsible for increasing the turbulence at the bottom, inducing a strong tangential flow and smearing the strong 8- cycle periodic flow, thus introducing a rather chaotic flow behaviour. Within this region, maximum values of the rms velocity of around 25% of the tip velocity were measured.

Further analysis of the data is required to extract various other useful quantities needed for assessing the performance of this impeller, such as the pump discharge coefficient and the distribution of the energy input into its various forms.

ACKNOWLEDGEMENTS

The authors wish to thank the European Commission and Junta Nacional de Investigação Científica e Tecnológica for financing this work through contracts JOU 2-CT9-0127 and PEAM/C/TAI/265/93, respectively. Special thanks are due to Mrs. Manuela Lemos for her assistance and valuable comments and to Mr. Jerónimo de Sousa for his technical support.